

# Temperature-Dependent Hyperfine Coupling Constant of the Dianion Radical of Fremy's Salt, a Convenient Internal Thermometer for EPR Spectroscopy

BARNEY L. BALES,\*† ELIANE WAJNBERG,‡ AND OTACIRO RANGEL NASCIMENTO\*

\*Departamento de Física and Informática, Instituto de Física de São Carlos, Universidade de São Paulo, 13560-970 São Carlos, Brazil; and ‡Centro Brasileiro de Pesquisas Físicas, 22290 Rio de Janeiro, Brazil

Received July 26, 1995; revised September 25, 1995

The hyperfine coupling constant,  $A_0$ , of peroxyamine disulfonate in aqueous solutions depends upon the temperature and the concentration of added  $K_2CO_3$  buffer. Near room temperature,  $A_0$  varies from 13.036 to 13.201 G for  $K_2CO_3$  concentrations varying from zero to near saturation. For samples prepared in 50.0 mM  $K_2CO_3$ , the results are independent of Fremy's salt concentration in the range 0.005–2.8 mM as follows:  $A_0(T) = 12.978 + 0.00311T$ , where the hyperfine coupling constant at temperature  $T$ ,  $A_0(T)$ , is given in gauss when the temperature is given in °C. This temperature dependence is an order of magnitude larger and of opposite sign than that found for doxylstearic acid esters and is proposed as the basis of an internal thermometer for EPR spectroscopy. The variation of  $A_0$  with solvent polarity is found to be a factor of about 27–30 less than for the neutral radicals di-*tert*-butyl nitroxide and doxylstearic acid esters. It is shown that microwave heating of aqueous samples at high microwave powers can be monitored by measuring  $A_0$  while conventional thermometry can lead to significant errors even for a thermocouple immersed within the sample just above the microwave cavity. The value of  $A_0(25^\circ C) = 13.056 \pm 0.002$  G is significantly different than previously used standards; therefore, some previous data may require recalibration. Correction procedures for nonlinearities in the field sweep are presented.

© 1996 Academic Press, Inc.

## INTRODUCTION

Fremy's salt, peroxyamine disulfonate (PADS), spontaneously forms the dianion radical ( $PADS^-$ ) upon dissolution into water or alcohol yielding a three-line, narrow EPR spectrum. The three lines are denoted by their values of the  $^{14}N$  spin quantum number,  $M_I = +1, 0$ , and  $-1$  corresponding respectively to the low-, middle-, and high-field lines. In addition to fundamental work (1–4), the spectrum has served as the basis for student experiments (5) and to calibrate magnetic fields. This latter function has been reported

to have been carried out innumerable times, often with no mention of the sample temperature. Thus, we were surprised to learn that the hyperfine coupling constant,  $A_0$ , of PADS shows a rather sizable temperature dependence in the range 0–70°C which does not seem to have been appreciated before, although it is known that  $A_0$  is temperature dependent in ice (2). Even though the careful measurement of Faber and Fraenkel (6) of  $A_0 = 13.0091 \pm 0.004$  G is quoted to be a measurement at  $T = 20^\circ C$ , in fact, the measurement was taken at an unspecified room temperature. Further, the sample was reported to have been prepared in saturated  $K_2CO_3$  rather than 50 mM  $K_2CO_3$  which is often used, and we have found that  $A_0$  depends upon the salt concentration.

We find a linear increase of  $A_0$  amounting to about 250 mG over the range 0–80°C, which, with modern EPR spectrometers, is sufficient to define the absolute temperature to  $\pm 1^\circ C$  in the range 0–40°C and  $\pm 1.4^\circ C$  up to 70°C and the relative temperature to  $\pm 0.5^\circ C$ .

The purpose of this work is as follows: (1) to report values of  $A_0$  for PADS under several well-defined conditions; (2) to report the temperature dependence of  $A_0$ ; and (3) to suggest its use as a thermometer for EPR spectroscopy. Most of the work deals with "standard" samples defined to be 0.005–2.8 mM PADS in 50.0 mM  $K_2CO_3$ , not degassed and sealed into a glass capillary; however, some data on the dependence of  $A_0$  on the concentration of  $K_2CO_3$  are given since this would permit recalibration of past data at concentrations other than 50.0 mM. Since our purpose is to provide data for practical uses of PADS as a standard,  $A_0$  is defined to be one-half the difference in the  $M_I = -1$  and  $+1$  resonance fields, is reported in magnetic field units, and is not corrected for small dynamic frequency shifts (7).

## EXPERIMENTAL

Fremy's salt from Alpha,  $K_2CO_3$  from Mallinckrodt, and ethanol, 95% Merck analytical grade, were used as received. Water was twice distilled from deionized water. The concen-

† On leave from the Department of Physics and Astronomy and the Center for Cancer and Developmental Biology, California State University at Northridge, Northridge, California 91330.

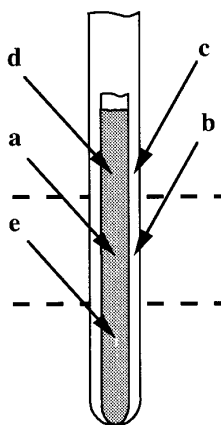


**FIG. 1.** Sample arrangement. A glass capillary filled with the solution is placed inside a quartz tube. The letters a–e indicate the locations of the thermocouple in various experiments. For placements c and b, the capillary is sealed at both ends and for a, d, and e, at the bottom only. The quartz tube is placed directly into the cavity or into a quartz nitrogen gas flow dewar.

trations of  $\text{PADS}^-$  were determined to  $\pm 20\%$  by comparison of the spectra with those of a freshly prepared sample of 16 doxylstearic acid ester in 100 mM aqueous solution of sodium dodecyl sulfate under identical conditions.

The resonance fields of the lines were established in two different ways. In the first, the positions were taken to be the point at which the first derivative lines crossed the base line which had been adjusted to give zero for the first integral of the spectrum. The crossover point was found by linear interpolation between the nearest two data points. In the second method, the resonance lines were fitted to a Voigt shape (8) using a fitting window  $\pm 3\Delta H_{pp}^0$ , where  $\Delta H_{pp}^0$  is the overall linewidth of the first-derivative line. These two determinations yielded the same line positions to within  $0.001 \pm 0.0004$  G and the same values of  $A_0$  to within  $0.00005 \pm 0.0002$  G. In other words, the difference in the interpolated crossover point and the center of a symmetrically fitted line is about 1 mG, and this difference is maintained from line to line in the spectrum, resulting in a negligible difference in  $A_0$  despite the fact that the resolution using 4096 data points is only on the order of 12 mG. Some experiments were run using 16,384 data points with no improvement in the reproducibility.

$A_0$  for a 0.25 mM PADS standard sample was measured on a Bruker ESP 300 E spectrometer equipped with an NMR gaussmeter. The sample capillary was placed inside a quartz tube as shown in Fig. 1. A copper-constantan thermocouple was placed inside the quartz tube in the position indicated by b in Fig. 1. Reproducible results on the standard sample were obtained by operating at room temperature,  $T_b = 20.5 \pm 0.2^\circ\text{C}$ , and sweeping the field through all three resonances. In this work, the subscript on temperatures indicates the position of the thermocouple. The magnetic fields at the

extremes of the sweep were measured with an NMR gaussmeter 17 times during the course of six EPR measurements and the average sweep width was used to calculate  $A_0$  for the standard sample yielding the results

$$A_0(20.5^\circ\text{C}) = 13.042 \pm 0.0023 \text{ G, standard sample} \quad [1]$$

where the quoted error is the standard deviation in six measurements taking into account the uncertainty in the sweep width.

Most of the work was carried out on a Varian E-109 X-band spectrometer with a field sweep generated by a microcomputer operating in MS-DOS using software written in the language C. The resulting sweep field still retained a small nonlinear component which was corrected using the methods given in the Appendix. The same card collected either 4096 or 16,384 data points at equal intervals of the sweep field. The field sweep was calibrated using the same standard reference sample producing Eq. [1]. The samples, not degassed, were drawn into glass capillaries which were sealed at both ends for thermocouple placements c and b, sealed at one end for placements a, d, and e, and placed inside a quartz tube (Fig. 1). The frequency was measured with a Hewlett–Packard 5352 B frequency counter at the beginning and at the end of each sweep, and a correction was made for the frequency variation using Eq. [22] of the Appendix.

The temperature was controlled with a Varian nitrogen flow unit. Only spectra in which the temperature was constant to within  $0.1^\circ\text{C}$  during the sweep were analyzed. The same thermocouple and Bailey Bat-9 readout unit were used in all of the measurements involving both spectrometers. The unit was calibrated in a well-stirred ice bath and at the boiling point of water corrected for local atmospheric pressure. The readouts in both baths were reproducible to  $\pm 0.1^\circ\text{C}$ . The linearity of the thermocouple unit was checked against two mercury-in-glass thermometers with a precision of  $0.1^\circ\text{C}$ , one in the range of  $0^\circ\text{C}$  calibrated in the same ice bath, and the other in the range  $100^\circ\text{C}$ , calibrated in the same boiling water. The accuracy of the temperatures reported here is estimated to be  $\pm 0.2^\circ\text{C}$ ; however, discrepancies between the temperature measured and the sample temperature can dominate the uncertainty for temperatures removed from room temperature depending upon where the thermocouple is located. Further, temperature gradients can become significant. With two thermocouples placed at points e and d, 1.5 cm apart, the average gradient was measured as a function of temperature. This average gradient, computed by dividing  $T_e - T_d$  by the 1.5 cm separation, reached  $\pm 0.2^\circ\text{C}/\text{cm}$  at temperatures  $\pm 13^\circ\text{C}$  from room temperature,  $0.3^\circ\text{C}/\text{cm}$  at  $40^\circ\text{C}$ , and  $0.8^\circ\text{C}/\text{cm}$  at  $70^\circ\text{C}$ .

The instrumental settings for Eq. [1] were as follows: time constant, 0.032 s; modulation amplitude, 0.1 G; sweep time,

**TABLE 1**  
**Temperature Dependence of  $A_0$**

$A_0(0)$ , G	$\frac{\partial A_0}{\partial T}$ ( $\times 10^4$ ), G/°C	Coefficient correlation <sup>a</sup>	Thermocouple position	Temperature range, °C
12.979	$31.3 \pm 0.2$	0.9996 (23)	a	0–70
12.980	$30.8 \pm 0.4$	0.9993 (9)	a	20–70
12.978	$31.9 \pm 0.5$	0.9977 (19)	a	20–70
12.976	$30.6 \pm 0.5$	0.9987 (19)	b	0–70
12.978	$31.0 \pm 0.5$	0.9990 (28)	c	0–40

Note.  $[K_2CO_3] = 50.0$  mM.  $[PADS] = 0.25$  mM.

<sup>a</sup> The number of measurements is given in the parentheses.

2 min; and microwave power, 2.0 mW. In a series of experiments, it was determined that the value of  $A_0$  was independent of these parameters up to these limits. This modulation amplitude broadened the lines affecting only the Gaussian component in agreement with the results of Ref. (9). The average Gaussian linewidth, determined as described in Ref. (9) produced by the over modulation was  $0.075 \pm 0.004$  G, independent of  $M_1$ , where the error is the standard deviation in the 18 lines from the six spectra used to yield Eq. [1].

## RESULTS

### Dependence of $A_0$ upon Temperature

The temperature dependence of  $A_0$  was determined with thermocouple placements a–d. First, it was ascertained that the presence of the thermocouple in the cavity does not affect  $A_0$  as follows: with a thermocouple immersed within the sample, the quartz tube was shifted back and forth so that positions a and d were alternately in the center of the cavity. The mean values in four measurements in each of the positions were within one-half of one standard deviation of all eight measurements which was 0.002 G. The measurements were fitted to a linear function as

$$A_0(T) = A_0(0) + \frac{\partial A_0}{\partial T} T. \quad [2]$$

The results are summarized in Table 1. Measurements using thermocouple positions b and c, after correcting the measured temperature, are given in the final two rows. The mean value of all measurements yields

$$A_0(T) = (12.978 \pm 0.0008) + (0.00311 \pm 0.00004)T. \quad [3]$$

In Eq [3],  $A_0(T)$  is in gauss when  $T$  is in °C. This is a rather large temperature dependence. For comparison, the temperature dependence of  $A_0$  for either 5- or 16-doxylstearic

acid ester in MeOH/H<sub>2</sub>O mixtures yields  $\partial A_0/\partial T = -0.00028 \pm 0.00002$  G/°C, an order of magnitude smaller than for PADS and of opposite sign. Figure 2 shows the results of all 98 measurements in Table 1; the solid line is Eq. [3]. The root-mean-square deviation of all of the measurements from Eq. [3] is 0.00036 G. The temperature may be deduced from a measurement of  $A_0(T)$  using Eq. [3]. The errors quoted in Eq. [3] are standard estimates ( $1\sigma$ ) from the linear least-squares fit. Since these data were derived from field sweeps calibrated by the standard sample, the uncertainty in Eq. [1], equivalent to  $\pm 0.7^\circ\text{C}$ , must be included in the uncertainty. For temperatures between 0 and  $40^\circ\text{C}$ , in which temperature gradients produce uncertainties of less than  $\pm 0.15^\circ\text{C}$ , the worst case estimate of the accuracy of Eq. [3] is  $\pm 1^\circ\text{C}$  which includes the uncertainty of  $\pm 0.2^\circ\text{C}$  in the thermocouple readout. Assuming the sources of uncertainty to be independent, the uncertainty in Eq. [3] in the range 0– $40^\circ\text{C}$  is dominated by the uncertainty in Eq. [1], i.e.,  $\pm 0.7^\circ\text{C}$ . Above  $40^\circ\text{C}$ , the uncertainty is difficult to assess in the absence of a more careful study of the effect of the temperature gradient; however, a worse case estimate is  $1.4^\circ\text{C}$  found by adding the maximum uncertainty of  $\pm 0.4^\circ\text{C}$  due to the gradient at  $70^\circ\text{C}$  to the above uncertainties.

The dianion radical in PADS is unstable, although we were able to use samples prepared in 50 mM  $K_2CO_3$  for several months if they were stored in the refrigerator. At higher temperatures, especially above  $60^\circ\text{C}$ , the signal degrades perceptibly within the 2 min sweep time. The values of  $A_0$  for PADS concentrations under 2.0 mM were not affected by these degradations as is expected from the results of the following section.

### Dependence of $A_0$ upon PADS Concentration

Spin exchange between PADS molecules leads to the well-known effect of reducing the distance between resonance lines

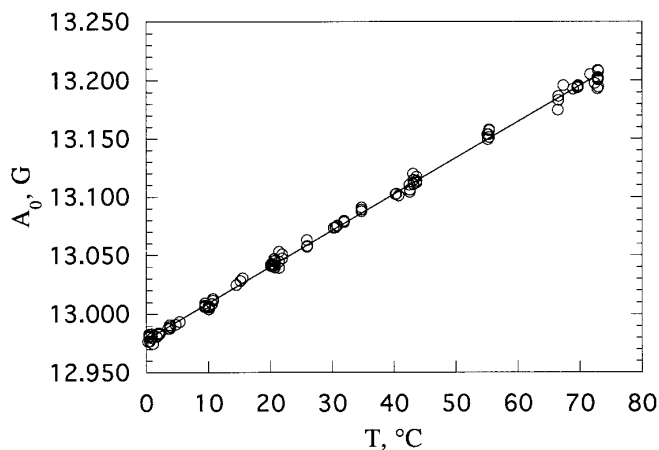


**FIG. 2.** The hyperfine coupling constant of the dianion radical of Fremy's salt vs temperature for samples prepared in 50.0 mM  $K_2CO_3$  aqueous solutions. These are the composite data for the five experiments summarized in Table 1 employing three different thermocouple placements. The line is a plot of Eq. [3].

**TABLE 2**  
 **$A_0$  vs PADS Concentration**

[PADS], mM	$T$ , °C	$A_0$ , <sup>a</sup> G
0.1	22.8 ± 0.1	13.038 ± 0.001 (3)
0.2	22.8 ± 0.1	13.035 ± 0.001 (3)
0.35	22.7 ± 0.2	13.037 ± 0.002 (3)
0.5	22.7 ± 0.2	13.036 ± 0.001 (3)
1.0	22.2 ± 0.1	13.036 ± 0.002 (4)
Mean	22.6 ± 0.3	13.036 ± 0.001 (16)

Note.  $[K_2CO_3] = 0$ .

<sup>a</sup> Measured by using an NMR gaussmeter. Errors are standard deviations in the number of measurements indicated in parentheses.

(11) which would appear as an apparent decrease in  $A_0$  according to our operational definition. Denote this decrease by  $(\delta A_0)_{ex} \leq 0$ . An advantage of using PADS as a standard is the fact that, due to the electrostatic repulsion between PADS molecules, this effect is small compared with that for most nitroxide spin probes (1). Jones (4) measured this effect, studying concentrations above 5 mM. Extracting data from Fig. 3 of Jones (4) on the linear relationship between [PADS] and the spin exchange frequency and using Jones' equations to back calculate the relationship between the spin exchange frequency and  $(\delta A_0)_{ex}$  show that  $(\delta A_0)_{ex}$  reaches  $(\delta A_0)_{ex} \approx 1.0$  mG for [PADS]  $\approx 2.8$  mM; thus, rather high concentrations of PADS may be used without need for correction for spin-exchange effects. Jones' results were obtained at  $T = 24^\circ\text{C}$  in samples prepared in 50 mM  $K_2CO_3$ . The value of  $(\delta A_0)_{ex}$  is expected to increase in magnitude with both  $[K_2CO_3]$  and temperature (1). Table 2 shows results at various PADS concentrations up to 1.0 mM and  $[K_2CO_3] = 0$ . Table 3 gives results up to [PADS] = 2.8 mM in samples of  $[K_2CO_3] = 50.0$  mM. At  $T$

**TABLE 3**  
 **$A_0$  vs PADS Concentration,  $[K_2CO_3] = 50.0$  mM<sup>a</sup>**

[PADS], mM	$A_0$ (25.2 ± 0.1°C) <sup>b</sup>	$A_0$ (62.8 ± 0.4°C)
0.38	13.055 ± 0.0003	
0.51	13.056 ± 0.0005	
0.64	13.057 ± 0.0004	
1.1	13.056 ± 0.0009	
1.3	13.056 ± 0.0003	13.175 ± 0.0016 (18) <sup>c</sup>
2.8	13.056 ± 0.0018	13.176 ± 0.0014 (20) <sup>d</sup>
Mean	13.056 ± 0.006	

<sup>a</sup> Field calibrated with standard sample. Values of  $A_0$  in gauss.

<sup>b</sup> Mean and standard deviation in four measurements.

<sup>c</sup> Measured over a period of 1.5 h as the signal decayed to 5.1% of its original intensity.

<sup>d</sup> Measured over a period of 1.8 h as the signal decayed to 0.81% of its original intensity.

<sup>c,d</sup> Mean values and standard deviations using the number of measurements indicated in parentheses.

**TABLE 4**  
 **$A_0$  vs  $[K_2CO_3]$**

$[K_2CO_3]$ , mM	$T$ , °C	$A_0$ , G
0	22.3 ± 0.3	13.035 ± 0.001 <sup>a</sup>
10.1	22.3 ± 0.3	13.039 ± 0.003 <sup>a</sup>
20.2	22.3 ± 0.3	13.040 ± 0.001 <sup>a</sup>
30.1	22.3 ± 0.3	13.043 ± 0.004 <sup>a</sup>
40.1	22.3 ± 0.3	13.045 ± 0.003 <sup>a</sup>
200	20.6 ± 0.1	13.059 ± 0.004 <sup>b</sup>
200	22.1 ± 0.1	13.067 ± 0.003 <sup>b</sup>
390	20.5 ± 0.1	13.073 ± 0.003 <sup>b</sup>
Saturated	20.2 ± 0.3	13.201 ± 0.003 <sup>b</sup>

Note. [PADS] = 0.25 mM.

<sup>a</sup> Measured by using an NMR gaussmeter.

<sup>b</sup> Measured using a field sweep calibrated by the standard sample.

= 22.6 or 25.2°C, the results are independent of [PADS] and the final rows of Tables 2 and 3 give the mean values of  $A_0$  for  $[K_2CO_3] = 0$  and  $[K_2CO_3] = 50.0$  mM, respectively.

Thus, for the purpose of field or temperature calibration, one does not need to be careful with the PADS concentration and can afford to prepare a sample with a very strong spectrum if needed. Certainly,  $A_0$  for 0.25 mM standard reference sample is negligibly affected by spin exchange.

#### Dependence of $A_0$ upon $K_2CO_3$ Concentration

Table 4 gives  $A_0$  vs  $[K_2CO_3]$  for samples with [PADS] = 0.25 mM. The final entry in Table 2 was determined from a sample prepared in saturated  $K_2CO_3$  which yielded a very weak spectrum due to the fact that PADS is only sparingly soluble at high  $K_2CO_3$ . This sample was prepared in an attempt to reproduce the reported conditions of Ref. (6). The spectrum (not shown) shows linewidth alteration typical of a nitroxide radical undergoing hindered rotation, undoubtedly due to the fact that such samples are quite viscous. The value of  $A_0 = 13.201$  G is significantly higher than the reported 13.091 G (6). Since, there was no mention of a weak signal or linewidth alteration in the original paper (6), the most likely source of the discrepancy is in the  $K_2CO_3$  concentration. From the data in Table 4, it is estimated that  $A_0 = 13.091$  G for  $[K_2CO_3] \approx 0.6$  M at  $T = 22.3^\circ\text{C}$ .

#### Dependence of $A_0$ upon Solvent

It is well known that the nitrogen hyperfine coupling constants of nitroxides depend upon the polarity of the solvent, correlating well with a number of empirical polarity parameters (12, 13). For nine solvents restricted to alcohols, water, and water-alcohol mixtures, Mukerjee *et al.* (13) showed that values of  $A_0$  for di-*tert*-butyl nitroxide were linear with the dielectric constant,  $D$ , as

$$A_0(D) = A_0(0) + \frac{\partial A_0}{\partial D} D, \quad [4]$$

**TABLE 5**  
 **$A_0$  vs Solvent**

Wt % EtOH	Dielectric constant <sup>a</sup>	$A_0$ (25°C)
0	78.5	13.047 ± 0.002 (5)
66.7	39.6	13.023 ± 0.002 (4)

Note.  $[K_2CO_3] = 12.5$  mM.  $[PADS] = 0.25$  mM.

<sup>a</sup> Ref. (15).

with  $r = 0.995$  and  $\partial A_0/\partial D = 0.0185$  G. Our own measurements of the 5- and 16-doxylstearic acid esters in MeOH/ $H_2O$  mixtures show that  $\partial A_0/\partial D$  is the same for the two nitroxides. The average of the results for the two doxylstearic acid esters is  $\partial A_0/\partial D = 0.0172 \pm 0.0004$  G. Measurement of  $A_0$  for PADS in water and an alcohol mixture gave the results in Table 5. From these data, the value of  $\partial A_0/\partial D$  is estimated to be  $\partial A_0/\partial D = 0.000627$  G, a factor of about 27–30 less than for the neutral radicals di-*tert*-butyl nitroxide and doxylstearic acid esters. These results are in accord with Ref. (14). Thus, PADS is rather insensitive to changes in the dielectric constant of the solution and the change in  $A_0$  with temperature cannot be attributed to changes in  $D$ ; in fact, the observed variation in Fig. 1 is opposite of that predicted by Eq. [4].

## DISCUSSION

The previously reported (6) value of  $A_0 = 13.091$  G is significantly higher than that measured for the standard sample at temperatures near room temperature, Eq. [1]; however, past data can be recalibrated provided the temperature and  $K_2CO_3$  concentration were reported.

Temperature measurement can be a problem in some experiments which makes Eq. [3] attractive in some cases. For example, in our setup at low microwave powers, we found the following: the difference in temperature at points b and c reached 3°C at 70°C and –3°C at 0°C. Even with thermo-

couples immersed within the sample, the difference in temperature between points a and d reached 1.4°C at low microwave powers. The difference between points inside and outside the capillary, a and b, reached 0.8°C at 70°C. At low powers, these measured temperatures are in agreement with the temperature calculated with Eq. [3] using measured values of  $A_0$ . Thus, in a setup in which the temperature is to be measured at a point removed from the sample, a sample of PADS measured at a low microwave power could be used to prepare a calibration curve of the measured temperature vs the sample temperature. It is fortunate that  $A_0$  is independent of PADS concentration to as high as 2.8 mM because a concentrated sample is needed to calibrate at high temperatures where the signal decays. One is able to work for about an hour and one-half at 60°C and about 20 min at 70°C starting with a 2.0 mM sample.

At higher microwave powers, which are used to carry out power-saturation experiments, microwave heating of aqueous samples becomes a problem. The results of four experiments are summarized in Table 6, three at room temperature and one with temperature control. At room temperature, with the thermocouple immersed in the sample in the center of the cavity, point a, the temperature calculated from Eq. [4] at a microwave power of 128 mW is about 4°C higher than the measured temperature, a difference that is probably not significant since the temperature profile is spatially dependent. The results with the thermocouple at point b are very similar to those with it at point a, so there is no need to immerse the thermocouple at room temperature. At 128 mW, the temperature measured with the thermocouple immersed within the sample but above the cavity, point d, is about 15°C lower than the temperature deduced from Eq. [4], demonstrating that significant temperature gradients that can be set up within the sample at high powers. Apparently, within the capillary, convection is insufficient to establish a uniform temperature; in fact, the sample heating ( $\approx 18^\circ C$ ) is barely detected ( $\approx 3^\circ C$ ) with the thermocouple at position d. With the temperature controlled at  $24.7 \pm 0.1^\circ C$ , the temperature of the sample still reaches  $36^\circ C$  at

**TABLE 6**  
**Microwave Heating of Aqueous PADS<sup>a</sup>**

Power mW	$T_a^{b,d}$	$T_a$ (Eq. [3])	$T_b^{b,e}$	$T_b$ (Eq. [3])	$T_c^{c,e}$	$T_c$ (Eq. [3])	$T_d^{b,d}$	$T_d$ (calc)
2	20.9 ± 0.1	21.1 ± 0.5	21.0 ± 0.1	21.0 ± 0.6	24.7 ± 0.1	24.8 ± 0.3	20.6 ± 0.1	20.3 ± 0.8
8			21.3 ± 0.1	21.8 ± 1.1	24.7 ± 0.1	25.3 ± 0.6		
32			23.9 ± 0.2	24.9 ± 1.1	25.2 ± 0.1	27.6 ± 1.1		
128	34.4 ± 0.1	38.8 ± 2.4	33.3 ± 0.6	38.7 ± 1.6	27.3 ± 0.1	36.0 ± 0.4	23.3 ± 0.1	38.1 ± 0.2

<sup>a</sup> Temperatures in °C.  $[PADS] = 0.25$  mM,  $[K_2CO_3] = 50.0$  mM. Errors are standard deviations in three measurements. The subscripts indicate thermocouple placement, Fig. 1, and  $T$  (Eq. [3]) is the temperature calculated from Eq. [3] from measured values of  $A_0$ .

<sup>b</sup> Room temperature.

<sup>c</sup> Temperature controlled at  $T = 24.7 \pm 0.1^\circ C$ .

<sup>d</sup> Without nitrogen gas flow dewar.

<sup>e</sup> With nitrogen gas flow dewar.

high powers while a thermocouple at position c detects only a 2°C rise in temperature. These results almost certainly depend upon the particular setup employed so the temperature vs power profile would need to be determined in each case. They do illustrate that the temperature rises significantly and is not easy to measure accurately. Fortunately, the temperature rise seems to be reproducible in a given setup. For example, in the three experiments at room temperature at 138 mW, the temperature as estimated using Eq. [3] was 38.8, 38.7, and 38.1°C (Table 6). This suggests that one could have success calibrating the temperature vs microwave power with a sample of PADS in a given setup and then replacing the PADS sample with the aqueous sample of interest. PADS gives a nice spectrum in alcohol/water mixtures, so samples of such mixtures could be prepared in order to study their microwave heating. The constants in Eq. [2] would need to be established in those cases first.

The above discussion involves using a separate sample of PADS as a thermometer. In samples in which PADS does not interfere chemically or spectrally, PADS could be incorporated into the sample and used as an internal thermometer after establishing the constants in Eq. [2]. In studies using  $^{14}\text{N}$  nitroxide spin probes,  $^{15}\text{N}$  PADS could be useful as an internal standard or in situations with the isotopes reversed.

## APPENDIX: SYSTEMATIC ERRORS

### Nonlinear Sweep Field

The magnetic field,  $B$  is given by

$$B = B_{\text{CF}} + V \text{SW}^*(a_0 + a_1V), \quad [5]$$

where  $B_{\text{CF}}$  is the center field,  $\text{SW}^*$  is the sweep width setting,  $V$  is a linear ramp that varies from  $-0.5$  to  $+0.5$ , and  $a_0$  and  $a_1$  are dimensionless constants. Equation [5] assumes that the nonlinearity is adequately described by a second-order polynomial. For a calibrated, linear field sweep,  $a_0 = 1$  and  $a_1 = 0$ . To calculate field differences,

$$\begin{aligned} B_2 - B_1 &= \text{SW}^*\{V_2(a_0 + a_1V_2) - V_1(a_0 + a_1V_1)\} \\ &= \text{SW}^*(V_2 - V_1)[a_0 + a_1(V_2 + V_1)], \quad [6] \end{aligned}$$

where the subscripts indicate the field positions and corresponding values of the ramp. Setting  $V_2 = 0.5$  and  $V_1 = -0.5$  shows that the true sweep width is  $\text{SW} = a_0 \text{SW}^*$ . If the field difference in Eq. [6] represents a hyperfine coupling constant, the true value  $A$  is given by

$$A = A^*[a_0 + a_1(V_2 + V_1)], \quad [7]$$

where  $A^* = \text{SW}^*(V_2 - V_1)$  is the apparent value.

For an  $^{14}\text{N}$  nitroxide radical, the spectrum has three lines defined by the values  $V_+$ ,  $V_0$ , and  $V_-$  corresponding to the

$M_I = +1, 0,$  and  $-1$ , respectively. Define the following measured separations of the lines of a nitroxide spectrum:

$$A_0^* = \text{SW}^*(V_- - V_+)/2 \quad [8]$$

$$A_{\pm}^* = \pm \text{SW}^*(V_0 - V_{\pm}). \quad [9]$$

The measured, apparent static second-order shift parameter is

$$\eta^* = A_{-}^* - A_{+}^*. \quad [10]$$

The asterisks in Eqs. [5]–[10] indicate that the quantities are those recorded which are in error if  $a_0 \neq 1$  and  $a_1 \neq 0$ . The correct value of the static second-order shift parameter is  $\eta = (A_0)^2/B_0$ . For  $B_0 = 3400$  G and  $A_0 = 13.057$  G,  $\eta = 50$  mG. Substituting the appropriate values of  $V_{M_I}$  into Eq. [7] gives expressions for  $A_0$ ,  $A_-$ , and  $A_+$ . From these, we find that

$$A_0 = A_0^*[a_0 + a_1(V_- + V_+)] \quad [11]$$

and

$$\eta = a_0\eta^* + a_1\{A_{-}^*(V_0 + V_-) - A_{+}^*(V_0 + V_+)\}. \quad [12]$$

Solving Eqs. [9] for  $V_+$  and  $V_-$  respectively and substituting into Eqs. [11] and [12] yields expressions for  $A_0$  and  $\eta$  which reduce to

$$A_0 = A_0^*\{a_0 + a_1(2V_0 + \eta^*/\text{SW}^*)\} \quad [13]$$

$$\begin{aligned} \eta &= a_0\eta^* + a_1\{2V_0\eta^* + (A_{-}^*)^2/\text{SW}^* \\ &\quad + (A_{+}^*)^2/\text{SW}^*\}. \quad [14] \end{aligned}$$

The terms  $a_1\eta^*/\text{SW}^*$  and  $a_12V_0\eta^*$  in Eqs. [13] and [14] are negligible and  $(A_{-}^*)^2 + (A_{+}^*)^2 = 2(A_0^*)^2$  to second order in  $\eta$ . Equations [13] and [14] then become

$$A_0 = A_0^*\{a_0 + 2a_1V_0\} \quad [15]$$

$$\eta = a_0\eta^* + 2a_1(A_0^*)^2/\text{SW}^*. \quad [16]$$

Suppose that the standard PADS sample, with known  $A_0$  from Eq. [3] and  $\eta = 50$  mG, is measured with the center line falling at  $V_0 = V_0(\text{cal})$ , yielding  $A_0^*(\text{cal})$  and  $\eta^*(\text{cal})$ . Equations [15] and [16] yield the constants  $a_0$  and  $a_1$  as

$$a_0 = \frac{(\eta V_0(\text{cal}) - A_0 A_0^*(\text{cal})/\text{SW}^*)}{\eta^* V_0(\text{cal}) - [A_0^*(\text{cal})]^2/\text{SW}^*} \quad [17]$$

$$a_1 = \frac{[\eta^* A_0 - \eta A_0^*(\text{cal})]}{2A_0^*(\text{cal})(\eta^* V_0(\text{cal}) - [A_0^*(\text{cal})]^2/\text{SW}^*)} \quad [18]$$

and Eq. [7] is used to correct  $A_0^*$ .

For convenience, redefine  $V_0(\text{cal}) = 0$  at the position of the center line of the standard sample during calibration. Thus, Eqs. [17] and [18] become

$$a_0 = A_0/A_0^*, \quad [19]$$

and

$$a_1 = \frac{(\eta - \eta^* a_0)}{2[A_0^*]^2/\text{SW}^*}, \quad [20]$$

For data taken with the center line at the same position as the center line of the standard, correction involves only multiplication by  $a_0$ , Eq. [19]. For positions  $V_0$  differing from the calibration position by  $\delta V_0$ , a further correction is needed which according to Eq. [15] is given by

$$\delta A_0 = 2A_0^* a_1 \delta V_0 = 2A_0^* a_1 \delta B_0/\text{SW}^*, \quad [21]$$

where  $\delta B_0/\text{SW}^* = \delta V_0$  corresponds to the field difference in the center line of the spectrum in question and the calibration point.

### Frequency Variation

After warm-up, the variation in the microwave frequency,  $\nu$ , was linear with the room temperature with  $\partial\nu/\partial T = -0.4$  MHz/°C. This variation is most likely due to fact that the AFC follows the decrease in cavity frequency as the cavity dimensions increase with temperature. Over a period of time in which 10–20 spectra are recorded, it was found that the room temperature and thus the frequency varied linearly with time; therefore, the variation during a given sweep,  $\delta\nu$ , may be taken as linear. If the field is swept up and the frequency changes by  $\delta\nu$ , then the frequency changes from the time the  $M_1 = +1$  resonance occurs until the  $M_1 = -1$  resonance occurs by  $2A_0\delta\nu/\text{SW}$ , where  $\nu$  is the average frequency, and

SW is the sweep field. This yields a resonance field at the  $M_1 = -1$  resonance that is in error by  $2A_0B_0\delta\nu/(\nu \text{SW})$  relative to its value for a constant frequency. Thus, the calculated  $A_0$  is in error by  $A_0B_0\delta\nu/(\nu \text{SW})$  and may be corrected by subtracting this value from  $A_0$ . If the field is swept downward, the correction needs to be added to  $A_0$ , so in general  $A_0$  is corrected as

$$A_0 = A_0^* - [\pm A_0 B_0 \delta\nu / (\nu \text{SW})], \quad [22]$$

where the plus and minus signs correspond to using an increasing or decreasing field sweep, respectively.

### ACKNOWLEDGMENTS

This work was supported by grants from the Fundação de Amparo À Pesquisa do Estado de São Paulo (FAPESP Project 94/1111-8) and the Conselho Nacional de Desenvolvimento Científico e Tecnológico (CNPq). Special thanks are due Dr. Cláudio Magon who dropped everything and installed the computer-controlled linear ramp and wrote the software.

### REFERENCES

1. M. P. Eastman, G. V. Bruno, and J. H. Freed, *J. Chem. Phys.* 52, 2511 (1970).
2. S. A. Goldman, G. V. Bruno, C. F. Polnaszek, and J. H. Freed, *J. Chem. Phys.* 56, 716 (1972).
3. S. A. Goldman, G. V. Bruno, and J. H. Freed, *J. Chem. Phys.* 59, 3071 (1973).
4. M. T. Jones, *J. Chem. Phys.* 38, 2892 (1963).
5. M. P. Eastman, *J. Chem. Ed.* 59, 677 (1982).
6. R. J. Faber and G. K. Fraenkel, *J. Chem. Phys.* 47, 2462 (1967).
7. G. K. Fraenkel, *J. Chem. Phys.* 42, 4275 (1965).
8. H. J. Halpern, M. Peric, C. Yu, and B. L. Bales, *J. Magn. Reson.* A 103, 13 (1993).
9. M. Peric and H. J. Halpern, *J. Magn. Reson.* A 109, 198 (1994).
10. P. R. Bevington, "Data Reduction and Error Analysis for the Physical Sciences," McGraw-Hill, New York, 1969.
11. Y. N. Molin, K. M. Salikhov, and K. I. Zamaraev, "Spin Exchange. Principles and Applications in Chemistry and Biology," Springer-Verlag, New York, 1980.
12. K. Mukai, H. Nishiguchi, K. Ishizu, Y. Deguchi, and H. Jakaki, *Bull. Chem. Soc. Jpn.* 40, 2731 (1967).
13. P. Mukerjee, C. Ramachandran, and R. A. Pyter, *J. Phys. Chem.* 86, 3189 (1982).
14. N. A. Malik, E. A. Smith, and M. C. R. Symons, *J. Chem. Soc. Faraday Trans.* 1 85, 3245 (1989).
15. G. Åkerlöf, *J. Am. Chem. Soc.* 54, 4125 (1932).